

Active control of an aircraft tail subject to harmonic excitation

M. Eissa · H. S. Bauomy · Y. A. Amer

Received: 4 April 2006 / Revised: 19 September 2006 / Accepted: 11 October 2006 / Published online: 8 June 2007
© Springer-Verlag 2007

Abstract Vibration of structures is often an undesirable phenomena and should be avoided or controlled. There are two techniques to control the vibration of a system, that is, active and passive control techniques. In this paper, a negative feedback velocity is applied to a dynamical system, which is represented by two coupled second order nonlinear differential equations having both quadratic and cubic nonlinearities. The system describes the vibration of an aircraft tail. The system is subjected to multi-external excitation forces. The method of multiple time scale perturbation is applied to solve the nonlinear differential equations and obtain approximate solutions up to third order of accuracy. The stability of the system is investigated applying frequency response equations. The effects of the different parameters are studied numerically. Various resonance cases are investigated. A comparison is made with the available published work.

Keywords Active vibration control · Stability · Response curves · Aircraft tail

1 Introduction

Vibration of a system or structure may cause disturbance, discomfort, damage, and destruction. For these reasons, one applies vibration control by using effective control tools.

The English text was polished by Keren Wang.

M. Eissa
Department of Engineering Mathematics,
Faculty of Electronic Engineering, Menouf 32952, Egypt

H. S. Bauomy (✉) · Y. A. Amer
Department of Mathematics, Faculty of Science,
Zagazig University, Zagazig, Egypt
e-mail: hany_samih@yahoo.com

Ricciardelli et al. [1] investigated the performance of active mass damper for the reduction of the buffet response of tall buildings. Eissa et al. [2,3] studied the control of both vibration and dynamics chaos of mechanical system having quadratic and cubic nonlinearities, subjected to harmonic excitation forces. Pai and Schulz [4] studied the control of the first mode vibration of a stainless steel beam through a negative velocity feedback. El-Badawy and Nayfeh [5] used two simple control laws based on linear velocity and cubic velocity feedback to suppress the high-amplitude vibrations of the twin-tail assembly of an F-15 fighter in a structural dynamic model when subjected to primary resonance excitations. Hanagud et al. [6] designed a standoff piezoceramic stack based active control system to control the fine vibrations of an F-15 tail. They found that as the disturbance level increases, the effectiveness of the controller decreases.

Shen et al. [7] used an actively constraining layer damping (ACLD) treatment, which consists of a piezoelectric constraining layer and a visco-elastic shear layer warping around the shaft in a helix form. They indicated that this method would reduce the vibration of the shaft. Fuller et al. [8] investigated active vibration control (AVC) with synthesis vibration source. Benassi et al. [9] used a frequency-domain formulation to analyze the stability and performance of an active isolation system using the modified inertial actuator and an outer velocity feedback control loop. Wu et al. [10] described the principle and application of AVC for reducing undesirable small-amplitude vertical vibration in the driver's seat of a vehicle. They used a frequency domain technique for achieving the control identification and controller design. Liu et al. [11] studied the vibration isolation characteristics of four semi-active damping control strategies, which are based on skyhook control and balance control. Eissa and Amer [12] studied the vibration control of a second order system simulating the first mode of a cantilever beam subjected to a

primary and sub-harmonic resonance. A control law based on cubic velocity feedback was proposed. Shih et al. [13] investigated the behavior of photostrictive opto-electromechanical actuators bonded to the surface of two-dimensional elastic structures for active vibration control. Pai et al. [14] presented a study on controlling steady-state vibrations of cantilevered skew aluminum plate using saturation phenomena due to higher-order-internal resonance. Omar et al. [15] designed a controller based on gain-scheduling feedback to move a load on a gantry crane from point to point within one oscillation cycle and without including large swings.

In the present paper, a two-degree-of-freedom system having quadratic and cubic nonlinearities subjected to multi-excitation forces is studied. The method of multiple time scale perturbation is used to solve the nonlinear differential equations describing the controlled system up to third order of accuracy. In this system, different active controllers are applied. The system is controlled by negative (linear, quadratic, cubic) velocity feedback. Best active control of the system is achieved by the negative velocity feedback. The stability of the system is investigated with frequency response equations. The resonance cases and effects of system's various parameters are studied numerically. A comparison is made with the available published work.

2 Mathematical analysis

The modified behavior of the twin-tail of an aircraft can be modeled in general by the following two generalized second-order coupled differential equations [5]:

$$\ddot{u}_1 + \omega_1^2 u_1 + 2\varepsilon\mu_1 \dot{u}_1 + \varepsilon\alpha_1 u_1^3 + \varepsilon\alpha_2 u_1^2 + \varepsilon\mu_3 \dot{u}_1 |\dot{u}_1| - \varepsilon\kappa(u_2 - u_1) = \varepsilon \sum_{S=1}^N F_S \cos(\Omega_S t + \tau_1) + R_1, \tag{1}$$

$$\ddot{u}_2 + \omega_2^2 u_2 + 2\varepsilon\mu_2 \dot{u}_2 + \varepsilon\alpha_3 u_2^3 + \varepsilon\alpha_4 u_2^2 + \varepsilon\mu_4 \dot{u}_2 |\dot{u}_2| - \varepsilon\kappa(u_1 - u_2) = \varepsilon \sum_{S=1}^N F_S \cos(\Omega_S t + \tau_2) + R_2, \tag{2}$$

where u_1, u_2 denote the generalized coordinates of the first bending modes of the twin-tail, ω_1, ω_2 are the lowest linear natural frequencies of the right and left tails, μ_1, μ_2 are the linear damping coefficients, α_1, α_3 are the coefficients of the cubic nonlinearity, α_2, α_4 are the coefficients of the quadratic nonlinearity, μ_3, μ_4 are the aerodynamic damping coefficients, F_s are the excitation amplitudes, Ω_s are the excitation frequencies, t is the time, τ_1, τ_2 are constants, ε is a small perturbation parameter, κ is the coupling coefficient of the twin tails, $R_1 = -\varepsilon G_1 \dot{u}_1^n$ and $R_2 = -\varepsilon G_2 \dot{u}_2^n$, ($n = 1, 2, 3$) are the control forces (linear, quadratic, cubic, respectively) and G_1, G_2 are positive constants, known as

the gains. In our investigation it is found that the best control law is the negative velocity feedback.

Assuming the solution of Eqs. (1) and (2) to be in the form

$$u_1(\varepsilon; t) = \sum_{n=0}^2 \varepsilon^n u_{1n}(T_0, T_1, T_2) + O(\varepsilon^3), \tag{3}$$

$$u_2(\varepsilon; t) = \sum_{n=0}^2 \varepsilon^n u_{2n}(T_0, T_1, T_2) + O(\varepsilon^3), \tag{4}$$

where $T_n = \varepsilon^n t$ ($n = 0, 1, 2$).

The derivatives will be in the form:

$$\frac{d}{dt} = D_0 + \varepsilon D_1 + \varepsilon^2 D_2, \tag{5}$$

$$\frac{d^2}{dt^2} = D_0 + 2\varepsilon D_0 D_1 + \varepsilon^2 (D_1^2 + 2D_0 D_2), \tag{6}$$

where $D_n = \frac{\partial}{\partial T_n}$, ($n = 0, 1, 2$)

Substituting Eqs. (3) and (4) into Eqs. (1) and (2) and grouping terms of the same power of ε , we have:

$$\varepsilon^0 : (D_0^2 + \omega_1^2)u_{10} = 0, \tag{7}$$

$$(D_0^2 + \omega_2^2)u_{20} = 0, \tag{8}$$

$$\begin{aligned} \varepsilon^1 : (D_0^2 + \omega_1^2)u_{11} = & -2D_0 D_1 u_{10} - 2\mu_1 (D_0 u_{10}) \\ & - \alpha_1 (u_{10}^3) - \alpha_2 (u_{10}^2) \mp \mu_3 (D_0 u_{10})^2 + \kappa (u_{20} - u_{10}) \\ & + \sum_{s=1}^N F_s \cos(\Omega_s t + \tau_1) - G_1 (D_0 u_{10}), \end{aligned} \tag{9}$$

$$\begin{aligned} (D_0^2 + \omega_2^2)u_{21} = & -2D_0 D_1 u_{20} - 2\mu_2 (D_0 u_{20}) \\ & - \alpha_3 (u_{20}^3) - \alpha_4 (u_{20}^2) \mp \mu_4 (D_0 u_{20})^2 + \kappa (u_{10} - u_{20}) \\ & + \sum_{s=1}^N F_s \cos(\Omega_s t + \tau_2) - G_2 (D_0 u_{20}), \end{aligned} \tag{10}$$

$$\begin{aligned} \varepsilon^2 : (D_0^2 + \omega_1^2)u_{12} = & -D_1^2 u_{10} - 2D_0 D_1 u_{11} - 2D_0 D_2 u_{10} \\ & - 2\mu_1 (D_1 u_{10} + D_0 u_{11}) - 3\alpha_1 (u_{10}^2 u_{11}) \\ & - 2\alpha_2 (u_{10} u_{11}) \mp 2\mu_3 (D_0 u_{10}) [(D_1 u_{10}) + (D_0 u_{11})] \\ & + \kappa (u_{21} - u_{11}) - G_1 (D_1 u_{10} + D_0 u_{11}), \end{aligned} \tag{11}$$

$$\begin{aligned} (D_0^2 + \omega_2^2)u_{22} = & -D_1^2 u_{20} - 2D_0 D_1 u_{21} - 2D_0 D_2 u_{20} \\ & - 2\mu_2 (D_1 u_{20} + D_0 u_{21}) - 3\alpha_3 (u_{20}^2 u_{21}) \\ & - 2\alpha_4 (u_{20} u_{21}) \mp 2\mu_4 (D_0 u_{20}) [(D_1 u_{20}) + (D_0 u_{21})] \\ & + \kappa (u_{11} - u_{21}) - G_2 (D_1 u_{20} + D_0 u_{21}). \end{aligned} \tag{12}$$

The general solutions of Eqs. (7) and (8) can be written in the form

$$u_{10}(T_0, T_1, T_2) = A_{10}(T_1, T_2) \exp(i\omega_1 T_0) + cc, \tag{13}$$

$$u_{20}(T_0, T_1, T_2) = A_{20}(T_1, T_2) \exp(i\omega_2 T_0) + cc, \tag{14}$$

where A_{10} , and A_{20} are complex functions and cc denotes the complex conjugate functions. Substituting Eqs. (13) and (14) into Eqs. (9) and (10), we get:

$$\begin{aligned}
 (D_0^2 + \omega_1^2)u_{11} = & -2i\omega_1[(D_1 A_{10}) \exp(i\omega_1 T_0)] \\
 & - 2i\omega_1\mu_1[A_{10} \exp(i\omega_1 T_0)] \\
 & - \alpha_1[A_{10}^3 \exp(3i\omega_1 T_0)] \\
 & + 3A_{10}^2(\bar{A}_{10}) \exp(i\omega_1 T_0)] \\
 & - \alpha_2[A_{10}^2 \exp(2i\omega_1 T_0) + A_{10}\bar{A}_{10}] \\
 & \pm \omega_1^2\mu_3[A_{10}^2 \exp(2i\omega_1 T_0) - A_{10}\bar{A}_{10}] \\
 & + \kappa[A_{20} \exp(i\omega_2 T_0) - A_{10} \exp(i\omega_1 T_0)] \\
 & + \frac{1}{2} \sum_{s=1}^N F_s \exp(i(\Omega_s T_0 + \tau_1)) \\
 & - i\omega_1 G_1 A_{10} \exp(i\omega_1 T_0) + cc, \tag{15}
 \end{aligned}$$

$$\begin{aligned}
 (D_0^2 + \omega_2^2)u_{21} = & -2i\omega_2(D_1 A_{20}) \exp(i\omega_2 T_0) \\
 & - 2i\omega_2\mu_2 A_{20} \exp(i\omega_2 T_0) \\
 & - \alpha_3[A_{20}^3 \exp(3i\omega_2 T_0)] \\
 & + 3A_{20}^2(\bar{A}_{20}) \exp(i\omega_2 T_0)] \\
 & - \alpha_4[A_{20}^2 \exp(2i\omega_2 T_0) + A_{20}\bar{A}_{20}] \\
 & \pm \omega_2^2\mu_4[A_{20}^2 \exp(2i\omega_2 T_0) - A_{20}\bar{A}_{20}] \\
 & + \kappa[A_{10} \exp(i\omega_1 T_0) - A_{20} \exp(i\omega_2 T_0)] \\
 & + \frac{1}{2} \sum_{s=1}^N F_s \exp(i(\Omega_s T_0 + \tau_2)) \\
 & - i\omega_2 G_2 A_{20} \exp(i\omega_2 T_0) + cc. \tag{16}
 \end{aligned}$$

Eliminating the secular terms in Eqs. (15) and (16), the general solution of the resulting equations is obtained as:

$$\begin{aligned}
 u_{11}(T_0, T_1, T_2) = & A_{11} \exp(i\omega_1 T_0) \\
 & + \frac{\alpha_1}{8\omega_1^2} A_{10}^3 \exp(3i\omega_1 T_0) \\
 & + \frac{\alpha_2}{3\omega_1^2} [A_{10}^2 \exp(2i\omega_1 T_0) - 3A_{10}\bar{A}_{10}] \\
 & \mp \mu_3 A_{10} \bar{A}_{10} \mp \frac{\mu_3}{3} A_{10}^2 \exp(2i\omega_1 T_0) \\
 & + \frac{\kappa}{(\omega_1^2 - \omega_2^2)} A_{20} \exp(i\omega_2 T_0) \\
 & + \sum_{s=1}^N F_s \left(\frac{\exp(i(\Omega_s T_0 + \tau_1))}{\omega_1^2 - \Omega_s^2} \right) + cc, \tag{17}
 \end{aligned}$$

$$\begin{aligned}
 u_{21}(T_0, T_1, T_2) = & A_{21} \exp(i\omega_2 T_0) \\
 & + \frac{\alpha_3}{8\omega_2^2} A_{20}^3 \exp(3i\omega_2 T_0) \\
 & + \frac{\alpha_4}{3\omega_2^2} [A_{20}^2 \exp(2i\omega_2 T_0) - 3A_{20}\bar{A}_{20}] \\
 & \mp \mu_4 A_{20} \bar{A}_{20} \mp \frac{\mu_4}{3} A_{20}^2 \exp(2i\omega_2 T_0) \\
 & + \frac{\kappa}{(\omega_2^2 - \omega_1^2)} A_{10} \exp(i\omega_1 T_0) \\
 & + \sum_{s=1}^N F_s \left(\frac{\exp(i(\Omega_s T_0 + \tau_2))}{\omega_2^2 - \Omega_s^2} \right) + cc. \tag{18}
 \end{aligned}$$

Similarly, substituting Eqs. (13), (14), (17) and (18) into Eqs. (11) and (12), we get

$$\begin{aligned}
 u_{12}(T_0, T_1, T_2) = & A_{12} \exp(i\omega_1 T_0) + E_1 \exp(i\omega_2 T_0) \\
 & + E_2 \exp(2i\omega_1 T_0) + E_3 \exp(2i\omega_2 T_0) \\
 & + E_4 \exp(3i\omega_1 T_0) + E_5 \exp(3i\omega_2 T_0) \\
 & + E_6 \exp(4i\omega_1 T_0) + E_7 \exp(5i\omega_1 T_0) \\
 & + E_8 \exp(i(\omega_1 + \omega_2)T_0) + E_9 \exp(i(\omega_2 + 2\omega_1)T_0) \\
 & + E_{10} \exp(i(\omega_2 - 2\omega_1)T_0) + E_{11} \exp(i(\omega_1 - \omega_2)T_0) \\
 & + E_{12} \exp(i(\Omega_s T_0 + \tau_1)) \\
 & + E_{13} \exp(i((\Omega_s + \omega_1)T_0 + \tau_1)) \\
 & + E_{14} \exp(i((\Omega_s - \omega_1)T_0 + \tau_1)) \\
 & + E_{15} \exp(i((\Omega_s + 2\omega_1)T_0 + \tau_1)) \\
 & + E_{16} \exp(i((\Omega_s - 2\omega_1)T_0 + \tau_1)) \\
 & + E_{17} \exp(i(\Omega_s T_0 + \tau_2)) + E_{18} + cc, \tag{19}
 \end{aligned}$$

$$\begin{aligned}
 u_{22}(T_0, T_1, T_2) = & A_{22} \exp(i\omega_2 T_0) + H_1 \exp(i\omega_1 T_0) \\
 & + H_2 \exp(2i\omega_2 T_0) + H_3 \exp(2i\omega_1 T_0) \\
 & + H_4 \exp(3i\omega_2 T_0) + H_5 \exp(3i\omega_1 T_0) \\
 & + H_6 \exp(4i\omega_2 T_0) + H_7 \exp(5i\omega_2 T_0) \\
 & + H_8 \exp(i(\omega_1 + \omega_2)T_0) + H_9 \exp(i(\omega_1 + 2\omega_2)T_0) \\
 & + H_{10} \exp(i(\omega_1 - 2\omega_2)T_0) + H_{11} \exp(i(\omega_2 - \omega_1)T_0) \\
 & + H_{12} \exp(i(\Omega_s T_0 + \tau_2)) \\
 & + H_{13} \exp(i((\Omega_s + \omega_2)T_0 + \tau_2)) \\
 & + H_{14} \exp(i((\Omega_s - \omega_2)T_0 + \tau_2)) \\
 & + H_{15} \exp(i((\Omega_s + 2\omega_2)T_0 + \tau_2)) \\
 & + H_{16} \exp(i((\Omega_s - 2\omega_2)T_0 + \tau_2)) \\
 & + H_{17} \exp(i(\Omega_s T_0 + \tau_1)) + H_{18} + cc, \tag{20}
 \end{aligned}$$

where, E_i and H_i , $i = 1, 2, \dots, 18$ are complex functions of T_1, T_2 .

So, the general solution of Eqs. (1) and (2) is

$$u_1(\varepsilon; t) = u_{10} + \varepsilon u_{11} + \varepsilon^2 u_{12} + o(\varepsilon^3), \tag{21}$$

$$u_2(\varepsilon; t) = u_{20} + \varepsilon u_{21} + \varepsilon^2 u_{22} + o(\varepsilon^3). \tag{22}$$

From Eqs. (21) and (22), the resonance cases are

- (1) Primary resonance: $\Omega_s = \omega_n, s, n = 1, 2$
- (2) Sub-harmonic resonance: $\Omega_s = m\omega_n, m = 2, 3, 4, 5, 6$
- (3) Internal resonance: $\omega_1 = r\omega_2$,
 $r = 1, 2, 3, 4, 5, \frac{1}{6}, \frac{1}{5}, \frac{1}{4}, \frac{1}{3}, \frac{1}{2}, \frac{3}{4}, \frac{3}{2}$
- (4) Combined resonance:
 - (i) $\Omega_1 \cong \omega_1 \pm \omega_2$
 - (ii) $\Omega_2 \cong \omega_1 \pm \omega_2$
 - (iii) $\Omega_1 \cong 2\omega_1 \pm \omega_2$
 - (iv) $\Omega_2 \cong 2\omega_1 \pm \omega_2$
 - (v) $\Omega_1 \cong \omega_1 \pm 2\omega_2$
 - (vi) $\Omega_2 \cong \omega_1 \pm 2\omega_2$

(5) Simultaneous resonance: Any combination of the above resonance cases is considered as a simultaneous resonance.

3 Stability analysis

The stability of the considered system is investigated at the worst resonance case (being confirmed numerically), which is the simultaneous primary resonance case where $\Omega_s \cong \omega_1$, $\Omega_s \cong \omega_2$.

Using the resonance conditions $\Omega_s = \omega_1 + \varepsilon\sigma_1$ and $\Omega_s = \omega_2 + \varepsilon\sigma_2$, then $\omega_2 = \omega_1 + \varepsilon\sigma_1 - \varepsilon\sigma_2$, where σ_1 and σ_2 are called the detuning parameters. Eliminating the secular terms from the first approximations of Eqs. (15) and (16) leads to solvability conditions as:

$$\begin{aligned}
 & -2i\omega_1 D_1 A_{10} - 2i\omega_1 \mu_1 A_{10} - 3\alpha_1 A_{10}^2 \bar{A}_{10} \\
 & + \frac{1}{2} \sum_{s=1}^N F_s \exp(i(\sigma_1 T_1 + \tau_1)) - i\omega_1 G_1 A_{10} \\
 & + \kappa [A_{20} \exp(i(\sigma_1 - \sigma_2) T_1) - A_{10}] = 0, \tag{23}
 \end{aligned}$$

$$\begin{aligned}
 & -2i\omega_2 D_1 A_{20} - 2i\omega_2 \mu_2 A_{20} - 3\alpha_3 A_{20}^2 \bar{A}_{20} \\
 & + \frac{1}{2} \sum_{s=1}^N F_s \exp(i(\sigma_2 T_1 + \tau_2)) - i\omega_2 G_2 A_{20} \\
 & + \kappa [A_{10} \exp(i(\sigma_2 - \sigma_1) T_1) - A_{20}] = 0. \tag{24}
 \end{aligned}$$

Using the polar form

$$A_{n0} = \frac{1}{2} a_n \exp(i\beta_n), \quad n = 1, 2, \tag{25}$$

where a_n and β_n are the steady state amplitudes and phases of the motions, respectively. Substituting Eq. (25) into Eqs. (23) and (24) and grouping the imaginary and real parts, we obtain:

$$\begin{aligned}
 & a'_1 + \mu_1 a_1 - \frac{1}{2\omega_1} F_s \sin \gamma_1 + \frac{1}{2} G_1 a_1 \\
 & - \frac{1}{2\omega_1} \kappa a_2 \sin \gamma_3 = 0, \tag{26}
 \end{aligned}$$

$$\begin{aligned}
 & a_1(\gamma'_1 - \sigma_1) + \frac{3\alpha_1}{8\omega_1} a_1^3 + \frac{1}{2\omega_1} \kappa a_1 \\
 & - \frac{1}{2\omega_1} F_s \cos \gamma_1 - \frac{1}{2\omega_1} \kappa a_2 \cos \gamma_3 = 0, \tag{27}
 \end{aligned}$$

$$\begin{aligned}
 & a'_2 + \mu_2 a_2 - \frac{1}{2\omega_2} F_s \sin \gamma_2 + \frac{1}{2} G_2 a_2 \\
 & + \frac{1}{2\omega_2} \kappa a_1 \sin \gamma_3 = 0, \tag{28}
 \end{aligned}$$

$$\begin{aligned}
 & a_2(\gamma'_2 - \sigma_2) + \frac{3\alpha_3}{8\omega_2} a_2^3 + \frac{1}{2\omega_2} \kappa a_2 \\
 & - \frac{1}{2\omega_2} F_s \cos \gamma_2 - \frac{1}{2\omega_2} \kappa a_1 \cos \gamma_3 = 0, \tag{29}
 \end{aligned}$$

where, $\gamma_1 = \sigma_1 T_1 - \beta_1 + \tau_1$, $\gamma_2 = \sigma_2 T_1 - \beta_2 + \tau_2$, and $\gamma_3 = \beta_2 - \beta_1 + \sigma_1 T_1 - \sigma_2 T_1$.

For steady-state solutions, $a'_n = \gamma'_n = 0$, $n = 1, 2$ and the periodic solution at the fixed points corresponding to Eqs. (24)–(27) is given by:

$$\mu_1 a_1 - \frac{1}{2\omega_1} F_s \sin \gamma_1 - \frac{1}{2\omega_1} \kappa a_2 \sin \gamma_3 + \frac{1}{2} G_1 a_1 = 0, \tag{30}$$

$$\begin{aligned}
 & \sigma_1 a_1 - \frac{3\alpha_1}{8\omega_1} a_1^3 - \frac{1}{2\omega_1} \kappa a_1 + \frac{1}{2\omega_1} F_s \cos \gamma_1 \\
 & + \frac{1}{2\omega_1} \kappa a_2 \cos \gamma_3 = 0, \tag{31}
 \end{aligned}$$

$$\mu_2 a_2 - \frac{1}{2\omega_2} F_s \sin \gamma_2 + \frac{1}{2\omega_2} \kappa a_1 \sin \gamma_3 + \frac{1}{2} G_2 a_2 = 0, \tag{32}$$

$$\begin{aligned}
 & \sigma_2 a_2 - \frac{3\alpha_3}{8\omega_2} a_2^3 - \frac{1}{2\omega_2} \kappa a_2 + \frac{1}{2\omega_2} F_s \cos \gamma_2 \\
 & + \frac{1}{2\omega_2} \kappa a_1 \cos \gamma_3 = 0. \tag{33}
 \end{aligned}$$

Squaring Eqs. (30) and (31) and taking summation, we obtain

$$\begin{aligned}
 & \frac{9\alpha_1^2}{64\omega_1^2} a_1^6 - \left(\frac{3}{4\omega_1} \alpha_1 \sigma_1 - \frac{3}{8\omega_1^2} \kappa \alpha_1 \right) a_1^4 \\
 & + \left(\mu_1^2 + \sigma_1^2 + \frac{1}{4} G_1^2 + \mu_1 G_1 + \frac{1}{4\omega_1^2} \kappa^2 - \frac{1}{\omega_1} \kappa \sigma_1 \right) a_1^2 \\
 & = \frac{1}{4\omega_1^2} [\kappa^2 a_2^2 + F_s^2 + 2\kappa F_s a_2]. \tag{34}
 \end{aligned}$$

Similarly, from Eqs. (32) and (33), we get:

$$\begin{aligned}
 & \frac{9\alpha_3^2}{64\omega_2^2} a_2^6 - \left(\frac{3}{4\omega_2} \alpha_3 \sigma_2 - \frac{3}{8\omega_2^2} \kappa \alpha_3 \right) a_2^4 \\
 & + \left(\mu_2^2 + \sigma_2^2 + \frac{1}{4} G_2^2 + \mu_2 G_2 + \frac{1}{4\omega_2^2} \kappa^2 - \frac{1}{\omega_2} \kappa \sigma_2 \right) a_2^2 \\
 & = \frac{1}{4\omega_2^2} [\kappa^2 a_1^2 + F_s^2 + 2\kappa F_s a_1]. \tag{35}
 \end{aligned}$$

From Eqs. (34) and (35), we have the following cases:

Case 1 $a_1 = a_2 = 0$: We obtain the trivial solution.

Case 2 $a_1 \neq 0, a_2 = 0$: In this case, the frequency response Eq. (34) is given by:

$$\begin{aligned}
 & \frac{9\alpha_1^2}{64\omega_1^2} a_1^6 - \left(\frac{3}{4\omega_1} \alpha_1 \sigma_1 - \frac{3}{8\omega_1^2} \kappa \alpha_1 \right) a_1^4 \\
 & + \left(\mu_1^2 + \sigma_1^2 + \frac{1}{4} G_1^2 + \mu_1 G_1 + \frac{1}{4\omega_1^2} \kappa^2 - \frac{1}{\omega_1} \kappa \sigma_1 \right) a_1^2 \\
 & = \frac{1}{4\omega_1^2} [F_s^2].
 \end{aligned}$$

Hence

$$\sigma_1 = \frac{1}{2} [\zeta_1 \pm (\zeta_2)^{\frac{1}{2}}]. \tag{36}$$

Case 3 $a_2 \neq 0, a_1 = 0$: In this case, the frequency response Eq. (35) is given by:

$$\begin{aligned} & \frac{9\alpha_3^2}{64\omega_2^2}a_2^6 - \left(\frac{3}{4\omega_2}\alpha_3\sigma_2 - \frac{3}{8\omega_2^2}\kappa\alpha_3\right)a_2^4 \\ & + \left(\mu_2^2 + \sigma_2^2 + \frac{1}{4}G_1^2 + \mu_2G_2 + \frac{1}{4\omega_2^2}\kappa^2 - \frac{1}{\omega_2}\kappa\sigma_2\right)a_2^2 \\ & = \frac{1}{4\omega_2^2}[F_s^2]. \end{aligned}$$

Hence

$$\sigma_2 = \frac{1}{2}[\zeta_3 \pm (\zeta_4)^{\frac{1}{2}}]. \tag{37}$$

Case 4 $a_1 \neq 0, a_2 \neq 0$: In this case, the frequency response equation is given by Eqs. (34) and (35), then:

$$\sigma_1 = \frac{1}{2}[\zeta_5 \pm (\zeta_6)^{\frac{1}{2}}], \tag{38}$$

$$\sigma_2 = \frac{1}{2}[\zeta_7 \pm (\zeta_8)^{\frac{1}{2}}], \tag{39}$$

where $\zeta_i, i = 1, \dots, 8$, are given in the appendix.

The steady state solution of the obtained fixed points of the linear system is determined as follows:

$$\begin{aligned} A_{n0} &= \frac{1}{2}(p_n - iq_n) \exp(i\sigma_n T_1); \\ &\text{where } p_n \text{ and } q_n \text{ are real; } n = 1, 2, \end{aligned} \tag{40}$$

$$\begin{aligned} & -2i\omega_1 A'_{10} - 2i\omega_1 \mu_1 A_{10} - i\omega_1 G_1 A_{10} \\ & + \kappa[A_{20} \exp(i(\sigma_1 - \sigma_2)T_1) - A_{10}] = 0, \end{aligned} \tag{41}$$

$$\begin{aligned} & -2i\omega_2 A'_{20} - 2i\omega_2 \mu_2 A_{20} - i\omega_2 G_2 A_{20} \\ & + \kappa[A_{10} \exp(i(\sigma_2 - \sigma_1)T_1) - A_{20}] = 0. \end{aligned} \tag{42}$$

Substituting Eq. (40) into Eqs. (41) and (42) and grouping the imaginary and real parts of Eqs. (41) and (42), we have:

$$p'_1 + \left(\mu_1 + \frac{G_1}{2}\right)p_1 + \left(\sigma_1 - \frac{\kappa}{2\omega_1}\right)q_1 + \frac{\kappa}{2\omega_1}q_2 = 0, \tag{43}$$

$$q'_1 + \left(\frac{\kappa}{2\omega_1} - \sigma_1\right)p_1 + \left(\mu_1 + \frac{G_1}{2}\right)q_1 - \frac{\kappa}{2\omega_1}p_2 = 0, \tag{44}$$

$$p'_2 + \left(\mu_2 + \frac{G_2}{2}\right)p_2 + \left(\sigma_2 - \frac{\kappa}{2\omega_2}\right)q_2 + \frac{\kappa}{2\omega_2}q_1 = 0, \tag{45}$$

$$q'_2 + \left(\frac{\kappa}{2\omega_2} - \sigma_2\right)p_2 + \left(\mu_2 + \frac{G_2}{2}\right)q_2 - \frac{\kappa}{2\omega_2}p_1 = 0. \tag{46}$$

The stability of a particular fixed point with respect to a perturbation proportional to $\exp(\lambda T_1)$ is determined by roots of the characteristic equation:

$$\begin{vmatrix} \lambda + \mu_1 + \frac{G_1}{2} & \sigma_1 - \frac{\kappa}{2\omega_1} & 0 & \frac{\kappa}{2\omega_1} \\ \frac{\kappa}{2\omega_1} - \sigma_1 & \lambda + \mu_1 + \frac{G_1}{2} & \frac{\kappa}{2\omega_1} & 0 \\ 0 & \frac{\kappa}{2\omega_2} & \lambda + \mu_2 + \frac{G_2}{2} & \sigma_2 - \frac{\kappa}{2\omega_2} \\ \frac{\kappa}{2\omega_1} & 0 & \frac{\kappa}{2\omega_2} - \sigma_2 & \lambda + \mu_2 + \frac{G_2}{2} \end{vmatrix} = 0. \tag{47}$$

To analyze the stability of the non-trivial solution, one uses Eq. (47) to obtain:

$$\lambda^4 + r_1\lambda^3 + r_2\lambda^2 + r_3\lambda + r_4 = 0, \tag{48}$$

where, r_1, r_2, r_3 and r_4 are constants given in the appendix.

According to the Routh-Hurwitz criterion, the necessary and sufficient conditions for all the roots of Eq. (48) to have negative real parts are:

$$\begin{aligned} & r_1 > 0, \quad r_1 r_2 - r_3 > 0, \\ & r_3(r_1 r_2 - r_3) - r_1^2 r_4 > 0 \quad \text{and} \quad r_4 > 0. \end{aligned}$$

4 Results and discussion

The Rung-Kutta fourth order method has been applied to determine the numerical solution of the given system. Figure 1 shows the non-resonant system behavior. It can be seen that the maximum steady state amplitudes of u_1 and u_2 are about 36 and 48% of the excitation force F_1 , respectively. This case can be regarded as a basic case.

4.1 Resonance cases

Figures 2, 3, 4, 5 and 6 show the response of the system at different resonance conditions. Table 1 shows the results of some of the worst resonance conditions. It describes the effect of the different worst resonance cases of the system before and after control. The worst resonance case of the system is the simultaneous primary resonance case, where $\Omega_1 \cong \Omega_2 \cong \omega_1 \cong \omega_2$. In this table we apply active control to all resonance cases and it is found that the amplitudes of the system are reduced. The effectiveness of the controller is represented by E_a = steady state amplitude of the system before control/steady state amplitude of the system after control.

4.2 Response curves and effects of different parameters

The frequency response Eqs. (36), (38) and (37), (39) are non-linear algebraic equations with respect to σ_1 and σ_2 . These equations are solved numerically as shown in Figs. 7, 8, 9 and 10. All these figures are bent to the right, which leads to multi-valued solutions and to jump phenomenon. There are stable (solid line) and unstable (dashed lines) solutions. For cases 2 and 3, that is, $a_1 \neq 0, a_2 \equiv 0$ and $a_2 \neq 0, a_1 \equiv 0$, respectively: Figs. 7 and 8 show that the steady state amplitudes of the system are increasing with the natural frequency of the right and left tails ω_1 and ω_2 , respectively, and the excitation coefficient F and decreasing with the nonlinear parameters α_1, α_3 , and the coupling coefficient κ . They are independent of the linear damping coefficients μ_1, μ_2 and the gains G_1, G_2 .

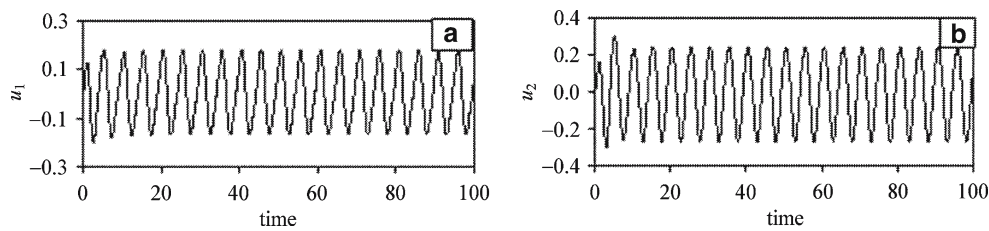


Fig. 1 Non-resonant case $\omega_1 \neq \omega_2 \neq \Omega_1 \neq \Omega_2$: $\mu_1 = 0.2$, $\alpha_1 = 0.004$, $\alpha_2 = 0.04$, $\mu_3 = 0.0004$, $\mu_2 = 0.3$, $\alpha_3 = 0.005$, $\alpha_4 = 0.05$, $\mu_4 = 0.0005$, $\omega_1 = 2.25$, $\omega_2 = 1.75$, $\Omega_1 = 1.25$, $\Omega_2 = 2.5$, $\kappa = 1.0$, $F_1 = 0.5$, $F_2 = 0.05$

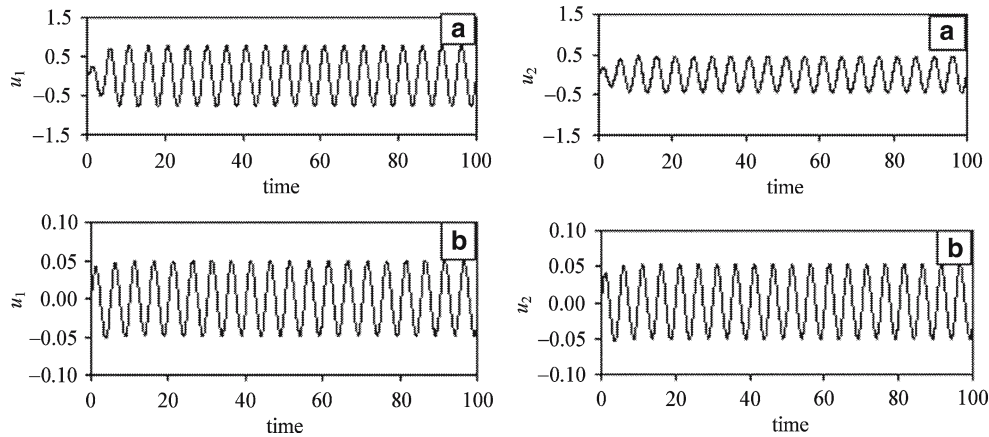


Fig. 2 Primary resonance case $\Omega_1 \cong \omega_1$. **a** Without controller; **b** with controller

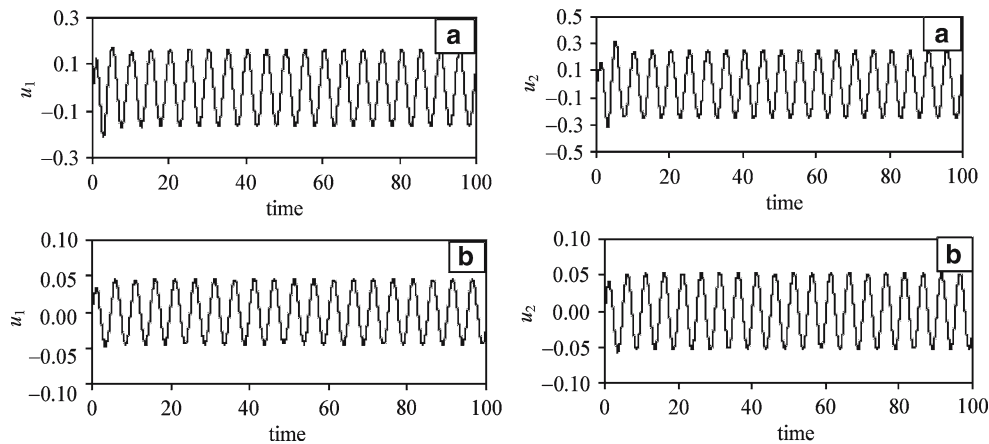


Fig. 3 Sub-harmonic resonance case $\Omega_2 \cong 3\omega_1$. **a** Without controller; **b** with controller

For case 4, where $a_1 \neq 0$, $a_2 \neq 0$: Figs. 9 and 10, show that the steady state amplitudes of the system are monotonically increasing with the natural frequency of the right tail ω_1 , the excitation coefficient F and decreasing with the non-linear parameters α_1 , α_3 , and the coupling coefficient κ , and also with the linear damping coefficients μ_1 , μ_2 and the gains G_1 , G_2 .

4.3 Vibration control

From Table 1 and Fig. 11, different types of resonance conditions are shown with the control. It can be seen that, the

steady state amplitudes of both modes can be controlled via a negative velocity feedback. Best results are obtained for the worst case (simultaneous primary resonance $\Omega_1 \cong \Omega_2 \cong \omega_1 \cong \omega_2$), where $E_a = 100$ for u_1 and $E_a = 50$ for u_2 , which means that u_1 is reduced to 1% and u_2 is reduced to 2%, respectively, with respect to their basic values. Figure 12 shows the results of the worst case which is simultaneous primary resonance $\Omega_1 \cong \Omega_2 \cong \omega_1 \cong \omega_2$, using both negative quadratic and cubic velocity feedbacks. It is clear that the best control method is the negative velocity feedback, where $E_a = 100$ for u_1 and $E_a = 50$ for u_2 at $n = 1$ (linear controller), $E_a = 8$ for u_1 and $E_a = 7$ for u_2 at $n = 2$

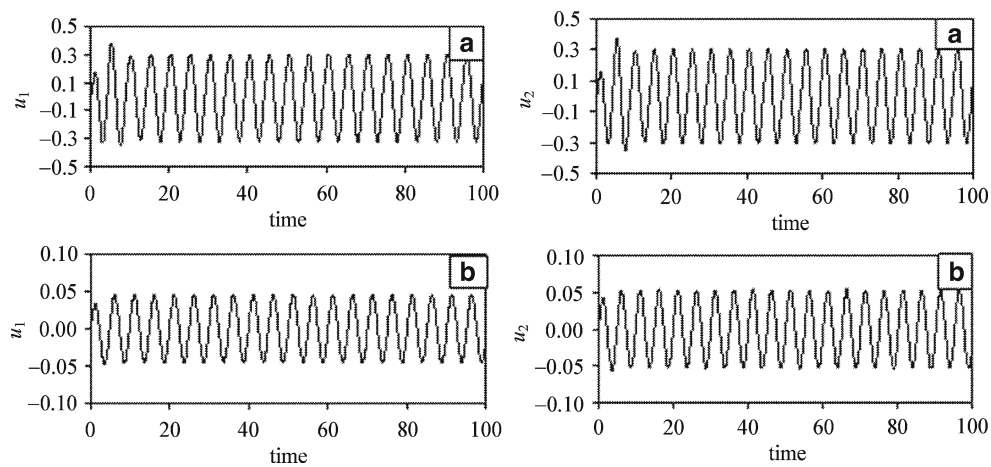


Fig. 4 Internal resonance case $\omega_1 \cong \omega_2$. **a** Without controller; **b** with controller

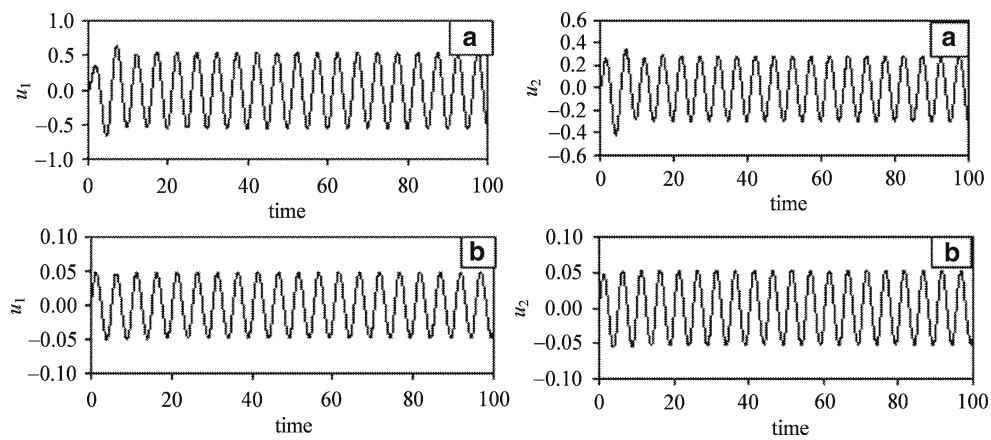


Fig. 5 Combined resonance case $\Omega_2 \cong \omega_1 + 2\omega_2$. **a** Without controller; **b** with controller

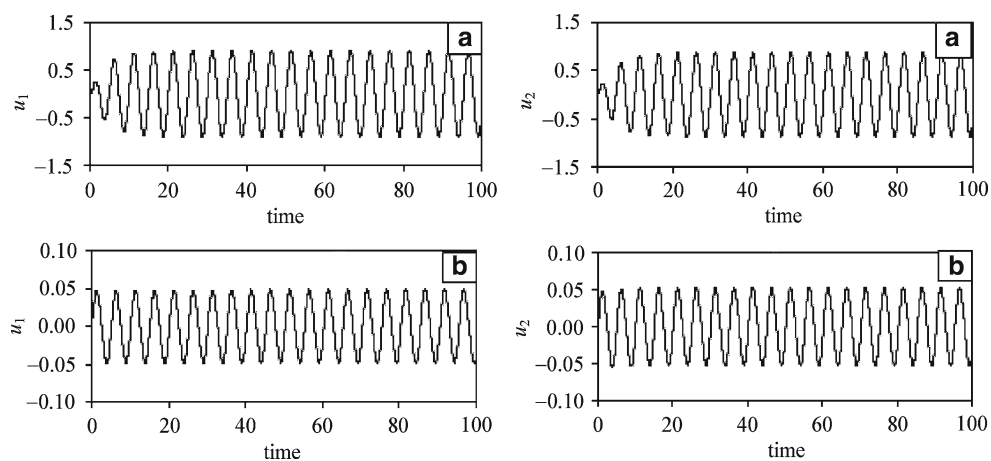
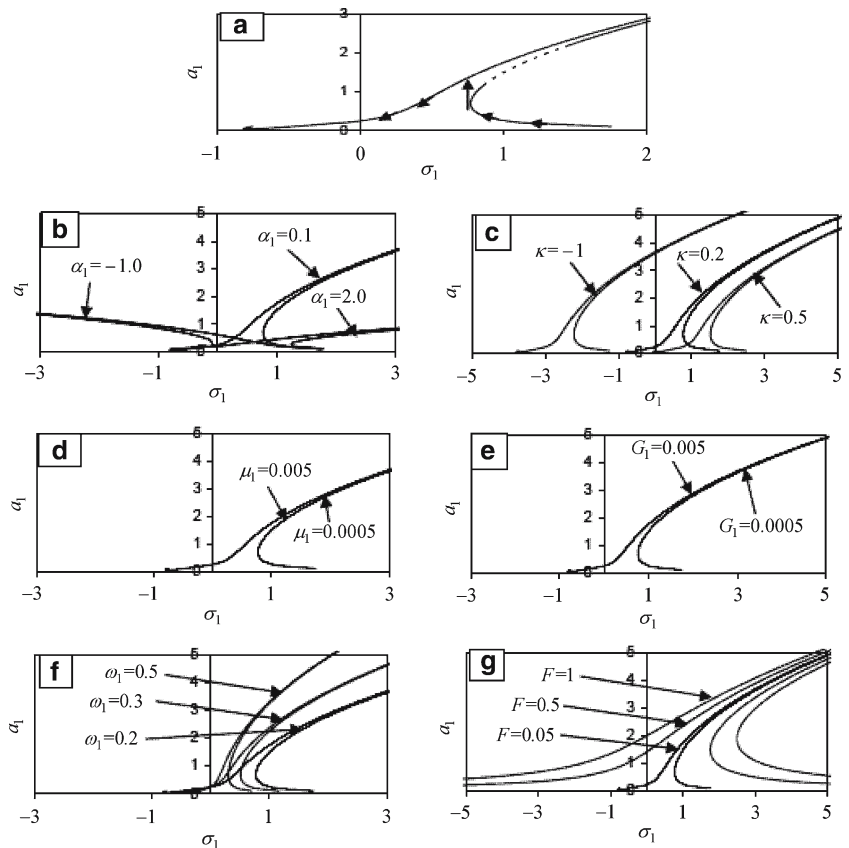


Fig. 6 Simultaneous resonance case $\Omega_1 \cong \Omega_2 \cong \omega_1 \cong \omega_2$. **a** Without controller; **b** with controller

Table 1 Summary of the worst resonance cases

Resonance cases	Without control		With control		Fig. no.	Remarks
	$u_1\%$	$u_2\%$	$u_1\%$	$u_2\%$		
Non-resonance $\omega_1 \neq \omega_2 \neq \Omega_1 \neq \Omega_2$	100	100	–	–	Fig. 1	Limit cycle
Primary resonance $\Omega_1 \cong \omega_1$	420	190	7 $E_a = 60$	10 $E_a = 20$	Fig. 2	Limit cycle
Sub harmonic resonance $\Omega_2 \cong 3\omega_1$	90	105	25 $E_a = 5$	20 $E_a = 5$	Fig. 3	Double limit cycle
Internal resonance $\omega_1 \cong \omega_2$	165	125	15 $E_a = 10$	15 $E_a = 10$	Fig. 4	Limit cycle
Combined resonance $\Omega_2 \cong \omega_1 + 2\omega_2$	300	120	8 $E_a = 40$	15 $E_a = 10$	Fig. 5	Limit cycle
Simultaneous primary resonance $\Omega_1 \cong \Omega_2 \cong \omega_1 \cong \omega_2$	500	380	5 $E_a = 100$	8 $E_a = 50$	Fig. 6	Limit cycle

Fig. 7 Response curves of the second case $a_1 \neq 0, a_2 = 0$. The basic case is: $\alpha_1 = 0.1, \kappa = 0.2, \mu_1 = 0.005, G_1 = 0.005, \omega_1 = 0.2, F = 0.05$



(quadratic controller), $E_a = 4$ for u_1 and $E_a = 4$ for u_2 at $n = 3$ (cubic controller).

5 Conclusions

The vibrations of a second order nonlinear system having both quadratic and cubic nonlinearities, subjected to multi-external excitation forces, can be controlled via a negative

feedback velocity to the system as in Refs. [4–6]. A multiple time scale perturbation method is used to determine approximate solutions for the coupled differential equations describing the system up to third order of accuracy. To study the stability of the system, both the frequency response equations and the phase-plane technique are applied. In Ref. [5], two controllers (linear and cubic velocity feedback) were applied to the system. They found that the linear velocity

Fig. 8 Response curves of the third case $a_2 \neq 0, a_1 = 0$. The basic case is: $\alpha_3 = 0.05, \kappa = 0.2, \mu_2 = 0.005, G_2 = 0.005, \omega_2 = 0.2, F = 0.05$

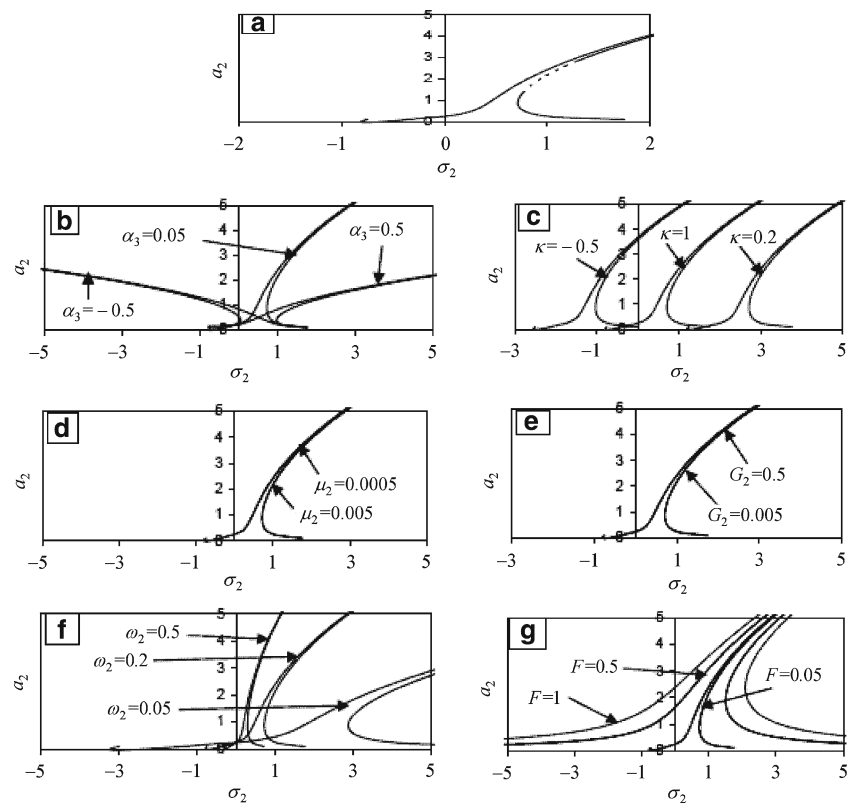


Fig. 9 Response curves of the fourth case $a_1 \neq 0, a_2 \neq 0$. The basic case is: $\alpha_1 = 0.1, \kappa = 0.2, \mu_1 = 0.005, G_1 = 0.005, \omega_1 = 0.2, F = 2.5$

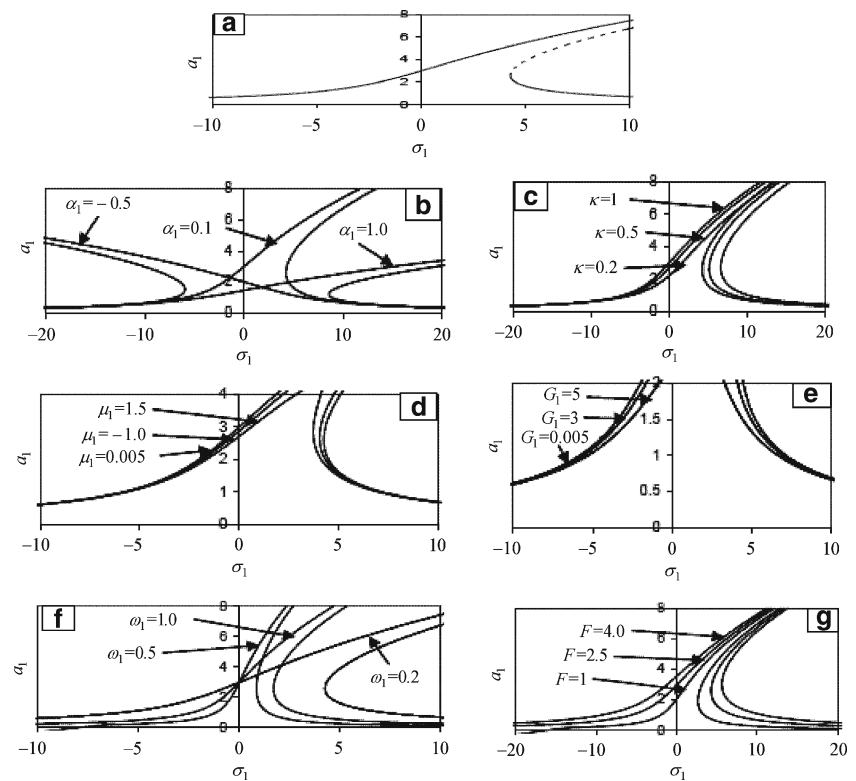


Fig. 10 Response curves of the fourth case $a_1 \neq 0, a_2 \neq 0$. The basic case is: $\alpha_3 = 0.1, \kappa = 0.2, \mu_2 = 0.05, G_2 = 2.0, \omega_2 = 0.2, F = 3.0$

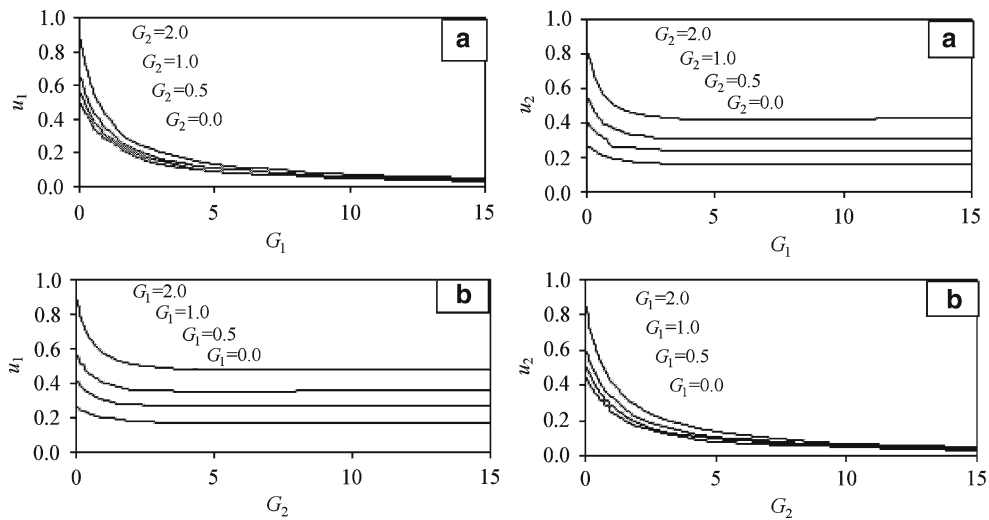
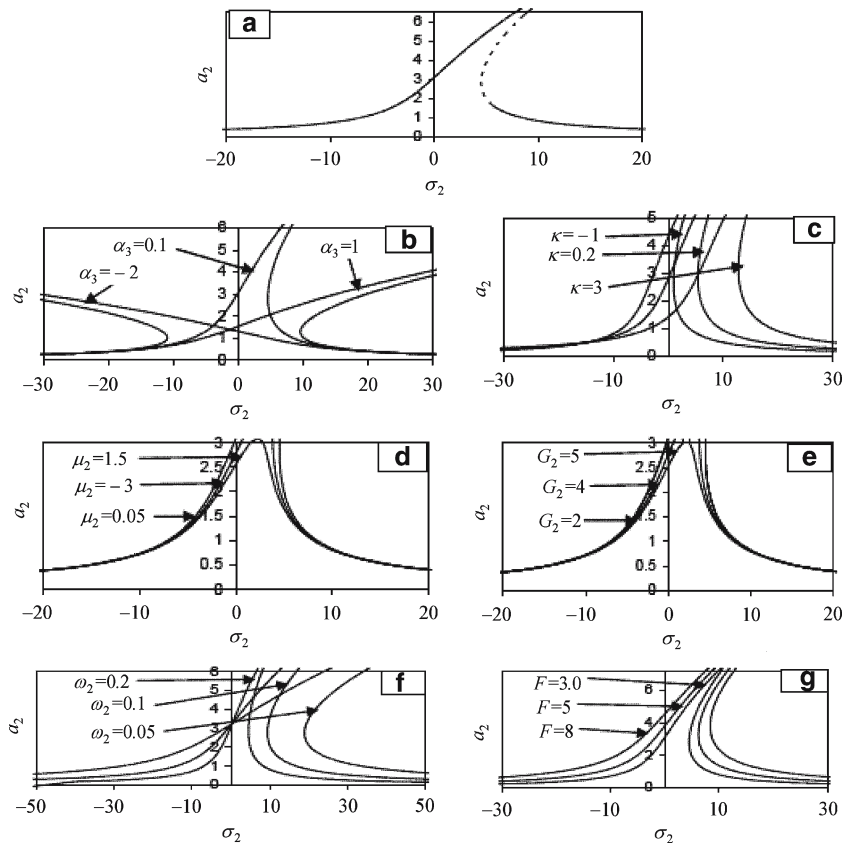
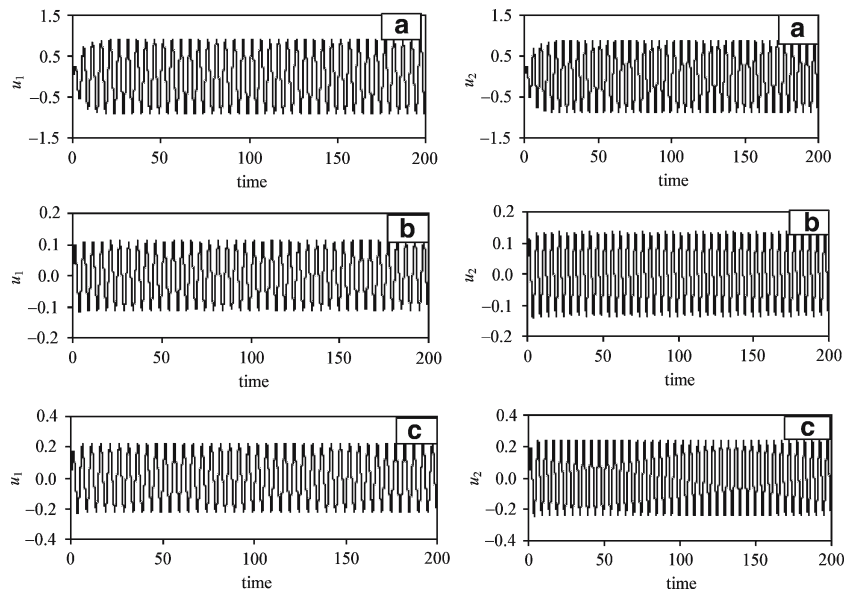


Fig. 11 Effect of the gains G_1 and G_2

feedback control is more effective than the cubic velocity feedback. From our study, the following may be concluded:

1. The worst resonance case of the system is the simultaneous primary case, where $\Omega_1 \cong \Omega_2 \cong \omega_1 \cong \omega_2$.
2. The effectiveness of the controller at the simultaneous primary resonance $\Omega_1 \cong \Omega_2 \cong \omega_1 \cong \omega_2$ is $E_a = 100$ and $E_a = 50$.
3. The steady state amplitudes of the system are monotonically increasing functions of the coefficients ω_1, ω_2 and F .
4. The steady state amplitudes of the system are monotonically decreasing functions of the coefficients $\alpha_1, \alpha_3, G_1, G_2$ and κ .
5. The steady state amplitudes of the system are independent of the linear damping coefficients α_1, α_3 and the

Fig. 12 Simultaneous resonance case $\Omega_1 \cong \Omega_2 \cong \omega_1 \cong \omega_2$. **a** Without controller; **b** with quadratic controller; **c** with cubic controller



gains G_1, G_2 in the cases of $a_1 \neq 0, a_2 = 0$ and $a_2 \neq 0, a_1 = 0$.

- 6. The steady state amplitudes u_1 and u_2 at the worst resonance case are monotonically decreasing functions of G_2 and G_1 , respectively, and the saturation occurs when $G_1 \geq 5$ and $G_2 \geq 5$, which agrees with Ref. [4].

Appendix

$$\zeta_1 = \frac{\kappa}{\omega_1} + \frac{3}{4\omega_1}\alpha_1 a_1^2,$$

$$\zeta_2 = \frac{F_s^2}{\omega_1^2 a_1^2} - 4\mu_1^2 - G_1^2 - 4\mu_1 G_1,$$

$$\zeta_3 = \frac{\kappa}{\omega_2} + \frac{3}{4\omega_2}\alpha_3 a_2^2,$$

$$\zeta_4 = \frac{F_s^2}{\omega_2^2 a_2^2} - 4\mu_2^2 - G_2^2 - 4\mu_2 G_2,$$

$$\zeta_5 = \frac{\kappa}{\omega_1} + \frac{3}{4\omega_1}\alpha_1 a_1^2,$$

$$\zeta_6 = \frac{F_s^2}{\omega_1^2 a_1^2} - 4\mu_1^2 - G_1^2 - 4\mu_1 G_1 + \frac{1}{\omega_1^2} \kappa^2 \frac{a_2^2}{a_1^2} + \frac{2}{\omega_1^2} \kappa F_s \frac{a_2}{a_1},$$

$$\zeta_7 = \frac{\kappa}{\omega_2} + \frac{3}{4\omega_2}\alpha_3 a_2^2,$$

$$\zeta_8 = \frac{F_s^2}{\omega_2^2 a_2^2} - 4\mu_2^2 - G_2^2 - 4\mu_2 G_2 + \frac{1}{\omega_2^2} \kappa^2 \frac{a_1^2}{a_2^2} + \frac{2}{\omega_2^2} \kappa F_s \frac{a_1}{a_2},$$

$$r_1 = 2\mu_2 + G_1 + G_2 + 2\mu_1,$$

$$r_2 = \mu_1^2 + \mu_2^2 + \frac{1}{4}G_1^2 + \frac{1}{4}G_2^2 + \mu_1 G_1 + \mu_2 G_2 + \sigma_1^2 + \sigma_2^2 + 4\mu_1 \mu_2 + \frac{\kappa^2}{4\omega_1^2} + \frac{\kappa^2}{4\omega_2^2} + \frac{\kappa^2}{2\omega_1 \omega_2} + G_1 G_2 + 2\mu_1 G_2 + 2\mu_2 G_1 - \frac{\kappa \sigma_2}{\omega_2} - \frac{\kappa \sigma_1}{\omega_1},$$

$$r_3 = 2\mu_1^2 \mu_2 + 2\mu_1 \mu_2^2 + \frac{1}{2}\mu_2 G_1^2 + \frac{1}{2}\mu_1 G_2^2 + \frac{1}{4}G_1^2 G_2 + \frac{1}{4}G_2^2 G_1 + 2\mu_1 \mu_2 G_2 + 2\mu_1 \mu_2 G_1 + G_1 \sigma_2^2 + G_2 \sigma_1^2 + 2\mu_1 \sigma_2^2 + 2\mu_2 \sigma_1^2 + \mu_2^2 G_1 + \mu_1^2 G_2 + \mu_2 G_1 G_2 + \mu_1 G_1 G_2 + \frac{1}{4\omega_2^2} \kappa^2 G_1 + \frac{1}{4\omega_1^2} \kappa^2 G_2 + \frac{\kappa^2 \mu_2}{4\omega_1 \omega_2} + \frac{\kappa^2 \mu_1}{4\omega_1 \omega_2} + \frac{\kappa^2 G_2}{4\omega_1 \omega_2} + \frac{\kappa^2 G_1}{4\omega_1 \omega_2} + \frac{1}{2\omega_1^2} \kappa^2 \mu_2 + \frac{1}{2\omega_2^2} \kappa^2 \mu_1 - \frac{2}{\omega_1} \kappa \sigma_1 \mu_2 - \frac{2}{\omega_2} \kappa \sigma_2 \mu_1 + \frac{\kappa^2}{4\omega_1 \omega_2} \mu_2 + \frac{\kappa^2}{4\omega_1 \omega_2} \mu_1 - \frac{\kappa G_1 \sigma_2}{\omega_2} - \frac{\kappa G_2 \sigma_1}{\omega_1},$$

and

$$r_4 = \mu_1^2 \mu_2^2 + \frac{1}{4}G_1^2 \mu_2^2 + \frac{1}{4}G_2^2 \mu_1^2 + \mu_2 \mu_1^2 G_2 + \mu_1 \mu_2^2 G_1 + \sigma_2^2 \mu_1^2 + \sigma_1^2 \mu_2^2 + \frac{\kappa^2}{4\omega_2^2} \mu_1^2 + \frac{\kappa^2}{4\omega_1^2} \mu_2^2 + \frac{1}{4}\mu_1 G_1 G_2^2 + \frac{1}{4}\mu_2 G_2 G_1^2 + \frac{1}{16}G_1^2 G_2^2$$

$$\begin{aligned}
& + \frac{\kappa^2}{2\omega_1\omega_2}\mu_1\mu_2 - \frac{\kappa}{\omega_1}\sigma_1\sigma_2^2 - \frac{\kappa}{\omega_2}\sigma_2\sigma_1^2 \\
& + \frac{\kappa^2}{4\omega_1\omega_2}\mu_2G_1 + \frac{\kappa^2}{4\omega_1\omega_2}\mu_1G_2 + \sigma_1^2\sigma_2^2 \\
& + \mu_2G_2\sigma_1^2 + \mu_1G_1\sigma_2^2 - \frac{\kappa}{\omega_2}\sigma_2\mu_1G_1 - \frac{\kappa}{\omega_1}\sigma_1\mu_2G_2 \\
& - \frac{\kappa\sigma_2\mu_1^2}{\omega_2} - \frac{\kappa\sigma_1\mu_2^2}{\omega_1} + \frac{\kappa^2\sigma_2^2}{4\omega_1^2} + \frac{\kappa^2\sigma_1^2}{4\omega_2^2} \\
& + \frac{1}{16\omega_2^2}\kappa^2G_1^2 + \frac{1}{16\omega_1^2}\kappa^2G_2^2 - \frac{\kappa}{4\omega_1}\sigma_1G_2^2 \\
& - \frac{\kappa}{4\omega_2}\sigma_2G_1^2 + \frac{\kappa^2\mu_1}{4\omega_2^2}G_1 + \frac{\kappa^2\mu_2}{4\omega_1^2}G_2 \\
& + \frac{\kappa^2}{8\omega_1\omega_2}G_1G_2 + \frac{\kappa^2}{2\omega_1\omega_2}\sigma_1\sigma_2 \\
& + \mu_1\mu_2G_1G_2 + \frac{1}{4}G_1^2\sigma_2^2 + \frac{1}{4}G_2^2\sigma_1^2.
\end{aligned}$$

References

1. Ricciardelli, F., Pizzimenti, A.D., Mattei, M.: Passive and active mass damper control of the response of tall buildings to wind gustiness. *Eng. Struct.* **25**, 1199–1209 (2003)
2. Eissa, M., El-Ganaini, W.A.A.: Multi-absorbers for vibration control of nonlinear structures to harmonic excitations. Part I, ISME Conference, Islamabad, Pakistan (2000)
3. Eissa, M., El-Ganaini, W.A.A.: Multi-absorbers for vibration control of nonlinear structures to harmonic excitations. Part II, ISME Conference, Islamabad, Pakistan (2000)
4. Pai, P.F., Schulz, M.J.: A refined nonlinear vibration absorber. *Int. J. Mech. Sci.* **42**, 537–560 (2000)
5. El-Badawy, A.A., Nayfeh A.H.: Control of a directly excited structural dynamic model of F-15 tail section. *J. Franklin Inst.* **338**, 33–147 (2001)
6. Hanagud, S., Patel, U., Robert, P., Henderson, D.: Control authority and the design of active control controller for buffet suppression. AIAA paper no. 1519 (2003)
7. Shen, I.Y., Guo, W., Pao, Y.C.: Torsional vibration control of a shaft through active constrained layer damping treatments. *ASME J. Vibr. Acoust.* **119**, 504–511 (1997)
8. Fuller, C.R., Elliott, S.J., Nelson, P.A.: *Active Control of Vibration*. Harcourt-Brace, Sandiego (1997)
9. Benassi, L., Elliott, S.J.: Active vibration isolation using an inertial actuator with local displacement feedback control. *J. Sound Vib.* **278**, 705–724 (2004)
10. Wu, J.D., Chen, R.J.: Application of an active controller for reducing small-amplitude vertical vibration in a vehicle seat. *J. Sound Vib.* **274**, 939–951 (2004)
11. Liu, Y., Water, T.P., Brennan, M.J.: A comparison of semi-active damping control strategies for vibration isolation of harmonic disturbances. *J. Sound Vib.* **280**, 21–39 (2005)
12. Eissa, M., Amer, Y.A.: Vibration control of a cantilever beam subject to both external and parametric excitation. *Appl. Math. Comput.* **152**, 611–619 (2004)
13. Shih, H.R., Tzou, H.-S., Saypuri, M.: Structural vibration control using spatially configured opto-electromechanical actuators. *J. Sound Vib.* **284**, 361–378 (2004)
14. Pai, P.F., Bernd, R.: Nonlinear vibration absorbers using higher-order-internal resonance. *J. Sound Vib.* **234**(5), 799–817 (2000)
15. Omar, H.M., Nayfeh, A.H.: Gantry gain scheduling feedback control with friction compensation. *J. Sound Vib.* **281**, 1–20 (2005)